

# LHD-Type Magnetic Configuration with Large Blanket Space<sup>\*)</sup>

Tsuguhiro WATANABE, Nagato YANAGI and Akio SAGARA

*National Institute for Fusion Science, Toki 509-5292, Japan*

(Received 18 November 2013 / Accepted 25 April 2014)

We studied the optimization of the magnetic configuration for the LHD-type fusion energy reactor (FFHR). We propose thin and flat helical coil systems, which are partitioned to three blocks with independent current value control, to satisfy the following requirements: (1) sufficient blanket space and large plasma volume under the helical coils with appropriate major radius and (2) divertor legs with little disorder that turn to the back of the helical coils. The cross-section of the plasma boundary changes from elliptical to racetrack-type. By extending the coil height, the coil current density of the central block for helical coil is observed to decrease gradually.

© 2014 The Japan Society of Plasma Science and Nuclear Fusion Research

Keywords: LHD, FFHR, configuration optimization, large blanket space

DOI: 10.1585/pfr.9.3403089

## 1. Introduction

The LHD-type magnetic configuration ( $\ell = 2$  heliotron configuration) is produced by continuous helical and vertical coil systems. LHD experiments obtained an average beta value of 5% without beta collapse. Based on the successful progress of fusion relevant plasma experiments, conceptual design studies on the LHD-type fusion energy reactors (FFHR) are being conducted both on physics and engineering issues [1–3]. In the design studies, the balance between blanket space ( $\equiv \delta$ : the narrowest space between the chaotic field lines outside the last closed flux surface (LCFS) and the inner wall of the helical coils) and plasma volume ( $\equiv V_{\text{lcfs}}$ : the volume enclosed by the LCFS) becomes an important issue. Several methods are proposed to clarify this issue, such as the  $\gamma$  (helical coil pitch parameter) value control of the helical coils [4, 5], splitting helical coil systems [6], and geodesic winding helical coil systems [7].

The main trend in helical magnetic configuration studies is based on the optimization of the spectrum of the magnetic field [8, 9]. Many sets of modular coils are determined by the optimized magnetic field [10]. In this case, the design of large opening ports, which is used for maintaining the in-core devices, becomes constrained. Furthermore, controlling the optimal magnetic field configuration in an operating fusion reactor plant is difficult.

In this study we use simplified continuous winding helical coils, which are split into three blocks. The optimization of the magnetic field is achieved by adjusting the current values of each coil block. Large opening ports for maintaining the in-core devices are possible. Controlling the core plasma under operation, such as the fusion output level and the temporary increase in the He ash exhaust, is

performed by simply regulating the coil current values.

The helical coils of the LHD are divided into three layers: the outside layer (H-O), the middle layer (H-M), and the inner layer (H-I). By controlling the current values of these coils, the LHD can change the helical pitch parameter  $\gamma$  defined by  $(m/\ell)(a_c/R_c)$  for continuous helical coils (having the toroidal pitch number  $m$ , poloidal pole number  $\ell$ , average minor radius  $a_c$ , and major radius  $R_c$ ):

$$1.1221 \leq \gamma_{\text{LHD}} \leq 1.3827.$$

The blanket space is increased by lowering  $\gamma$ , which also causes the plasma volume  $V_{\text{lcfs}}$  to decrease.

In the present paper, we propose a thin and flat helical coil system with current distribution control. The helical coil is divided into three blocks parallel to each other. Magnetic field parameters, such as the field intensity  $B_{\text{ax}}$  on the magnetic axis and the total magnetic energy  $W_B$ , are determined by the total ampere-turns of the helical coil. Nonetheless, the perturbed magnetic field component near the LCFS can be actively controlled by the current distribution of the helical coils. Therefore, we can change the magnetic surface form into the racetrack-type. Large blanket space and large plasma volume become compatible by adjusting the combination of helical coil current values.

In Sec. 2, we describe the relation between the blanket space, plasma volume, and structure of the divertor leg, using a straight helical system. We also show the strong positional stability of the magnetic surface and divertor legs, which turn to the back of the helical coils. In Sec. 3, we describe the magnetic configuration with large blanket space and large plasma volume. We discuss the results in Sec. 4.

## 2. Blanket Space and Plasma Volume in Helical System

Using a straight helical system, we show in Fig. 1 that three types of magnetic surfaces exist in a helical magnetic

author's e-mail: watanabe.tsuguhiro@toki-fs.jp

<sup>\*)</sup> This article is based on the presentation at the 23rd International Toki Conference (ITC23).

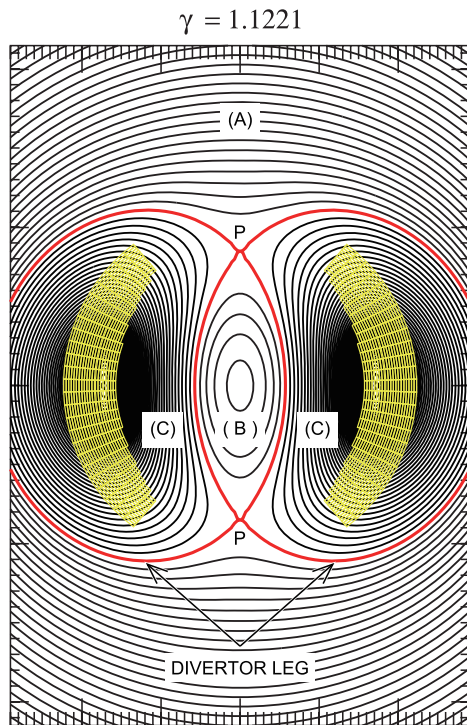


Fig. 1 Magnetic surface of the straight helical system.

field produced by continuous winding  $\ell = 2$  helical coils. Type (A) magnetic surface encloses the two helical coils. Type (C) magnetic surface encloses each helical coil. The separatrix between (A) and (C) are the divertor legs, which positionally have a very stable structure and turn to the back of the helical coils. In the toroidal system, the lines of force near the null points (P) become chaotic and  $V_{\text{LCFS}}$  decreases slightly, depending on the configuration of the vertical magnetic field. Type (B) magnetic surface (magnetic surface for the core plasma) is sandwiched between the type (C) magnetic surfaces. Thus, the plasma volume and the blanket space have a trade-off relation. This figure also shows that as the height of the helical coil increases, it strengthens the interference of the helical coil and divertor leg.

Figure 2 shows the modification of the LHD magnetic surface using the  $\gamma$  value control. The standard configuration ( $\gamma = 1.2538$ ) of the LHD has sufficient plasma volume ( $V_{\text{LCFS}} = 28.6 \text{ m}^3$ ), but the blanket space is very narrow ( $\delta = 0.171 \text{ m}$ ), as shown in Fig. 2(a). The smallest  $\gamma$  configuration ( $\gamma = 1.1221$ ) of the LHD has sufficient blanket space ( $\delta = 0.32 \text{ m}$ ), but the plasma volume is very small, as shown in Fig. 2(b). By adjusting the magnetic axis position to the optimal value, the plasma volume  $V_{\text{LCFS}}$  of the standard configuration becomes 94.85% of the corresponding straight helical system in Fig. 1. However, the volume of the smallest  $\gamma$  configuration decreases by no less than 38.4% compared with the volume of the standard configuration.

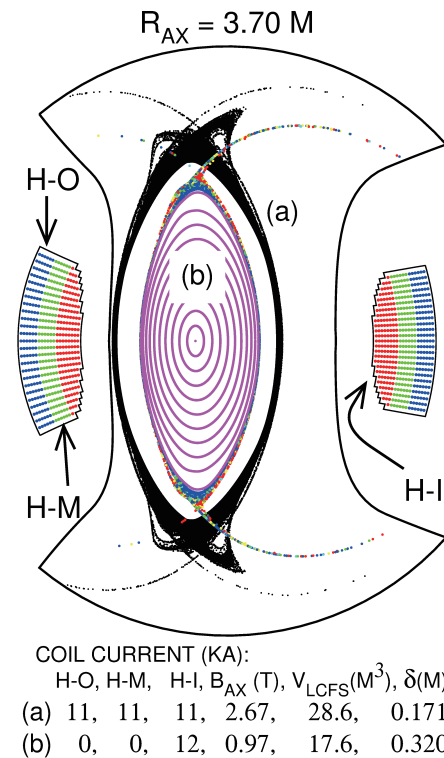


Fig. 2 An example of the modification of the LHD magnetic surface using the  $\gamma$  value control. (a) One of the standard magnetic surface with  $\gamma = 1.2538$  obtained at equal current values for each helical coil winding H-O, H-M, and H-I. (b) The smallest  $\gamma$  value (1.1221) magnetic surface obtained by using the H-I winding only.  $V_{\text{LCFS}}$  and  $\delta$  are the plasma volume and the blanket space, respectively.

### 3. Magnetic Configuration with Large Blanket Space and Large Plasma Volume

To increase the plasma volume  $V_{\text{LCFS}}$  while keeping the blanket space  $\delta$  constant, changing the shape of the magnetic surface from elliptical to racetrack-like is necessary. Therefore, we proposed a thin and flat helical coil as shown in Fig. 3. The helical coil is partitioned to three blocks: HC-I, HC-II, and HC-III, with independent current values.

Because the helical pitch parameter of the central helical coil block HC-I shown in Fig. 3 is small, i.e.,

$$\gamma_{\text{HC-I}} = \frac{5 \times 0.896}{3.9} = 1.14871 \dots,$$

large blanket space  $\delta$  is expected. However, the magnetic surface produced by the H-I coil is convex to the helical coil (elliptical cross-section), as shown in Fig. 2, and thus the plasma volume is small. The magnetic surface becomes concave to the helical coil by feeding a strong negative current to the helical coil HC-II, which is placed on both sides of the HC-I. Too strong concave structure of the magnetic surface causes the interference of the divertor legs with the ends of the helical coils. Therefore, we make the magnetic surface take the shape of a racetrack and increase the plasma volume by feeding the appropriate

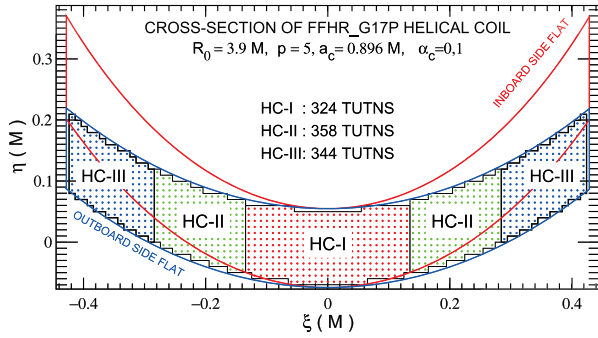


Fig. 3 The thin and flat helical coil is shown in the LHD scale.  $(\xi, \eta)$  is the plane perpendicular to the helical coil.  $\eta$  is the radial direction from the helical coil center. The blue and red lines show the vertical lines at the outboard and inboard side. The center of the helical coil  $(0, 0)$  is wound on the circular ring with minor radius  $a_c$  with helical coil pitch modulation factor  $\alpha_c = 0.1$ .

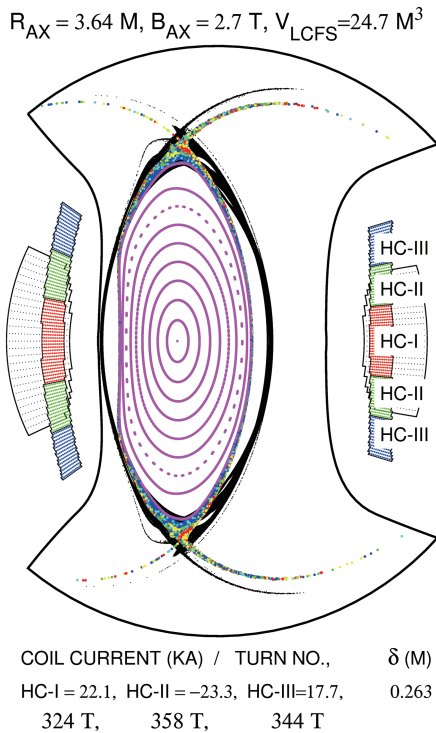


Fig. 4 Racetrack-type magnetic surface. For comparison, the standard magnetic surface ( $R_{ax} = 3.65$  m) and helical coils of the LHD are also shown in black.

negative current to the HC-II coil. Positive current is set to the HC-III block to make clearance between the helical coils and divertor legs.

Figure 4 compares the racetrack-type magnetic surface, which is generated by the thin and flat helical coil in Fig. 3, and the LHD standard magnetic surface. The racetrack-type magnetic surface shows that the decrease in plasma volume can be reduced while ensuring the blanket space.

A numerical example of the magnetic field with large

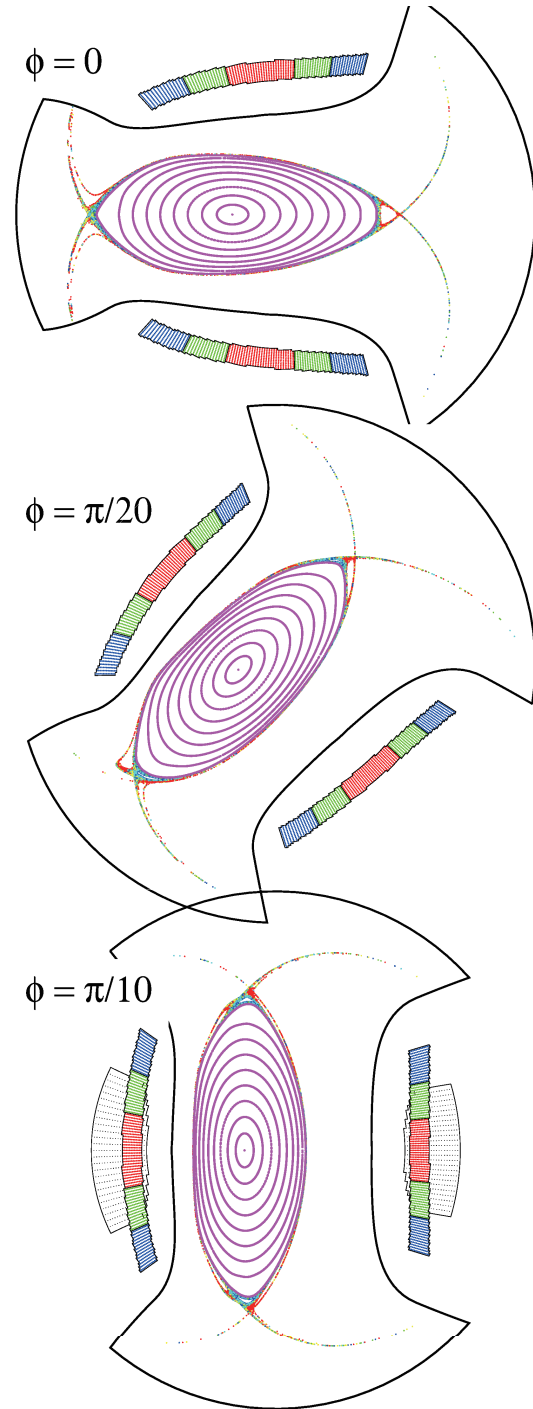


Fig. 5 Magnetic field configuration with large blanket space and large plasma volume. Helical coils (only for the toroidal angle  $\phi = \pi/10$ ) and vacuum vessel that are similar extension of the LHD are also shown.

Table 1 Coil parameters for the case of Fig. 5 with  $R_0 = 16.7$  m and  $B_{ax} = 5$  T. ( $\delta$ : blanket space,  $V_{lcf}$ : plasma volume).

	HC-I	HC-II	HC-III	$\delta / V_{lcf}$
$I$ (MA)	61.4	-38.0	16.0	1.385 m
$J_c$ (A/mm <sup>2</sup> )	103.4	-57.9	25.4	1731.8 m <sup>3</sup>

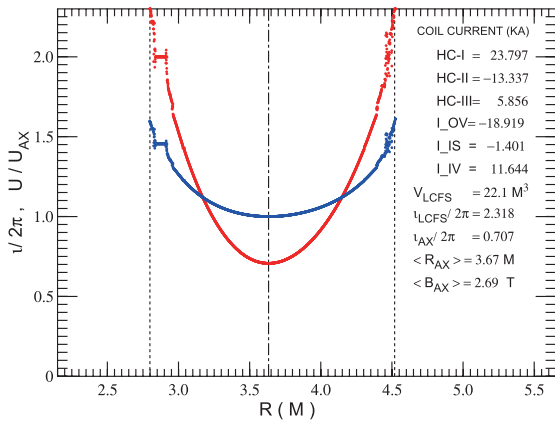


Fig. 6 Distributions of the specific volume  $U$  (blue) and the rotational transform  $\nu/2\pi$  (red).

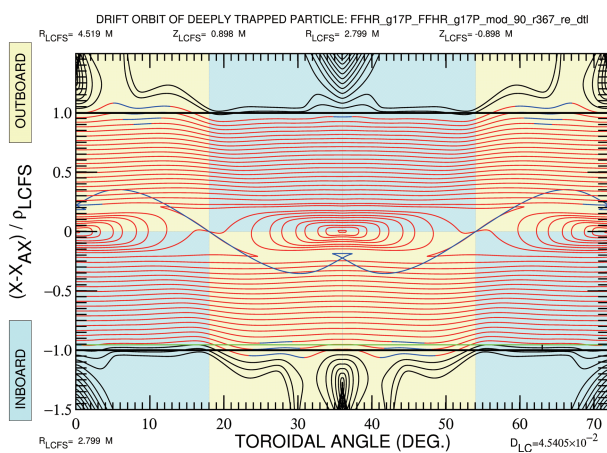


Fig. 7 Trapped orbits diagram. The horizontal axis is the toroidal angle. The vertical axis  $X$  is the rotating helical coordinate along the long axis of the magnetic surface.  $X_{ax}$  is the position of the magnetic axis and  $\rho_{lcfs}$  is the minor radius of the LCFS.

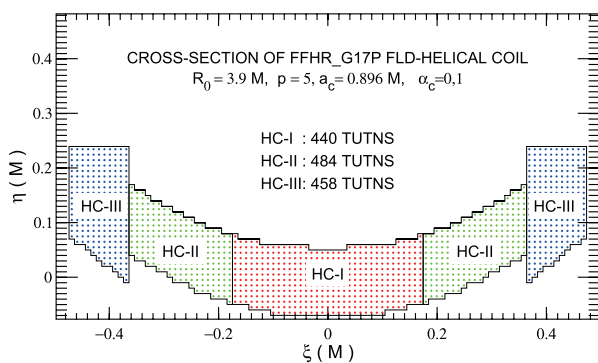


Fig. 8 Folded-type thin and flat helical coil.

blanket space and large plasma volume for a helical reactor is shown in Fig. 5. The coil current data are summarized in Table 1. The distributions of the specific volume  $U$  and the rotational transform  $\nu/2\pi$  are shown in Fig. 6 (using the LHD machine size). A magnetic well is not present

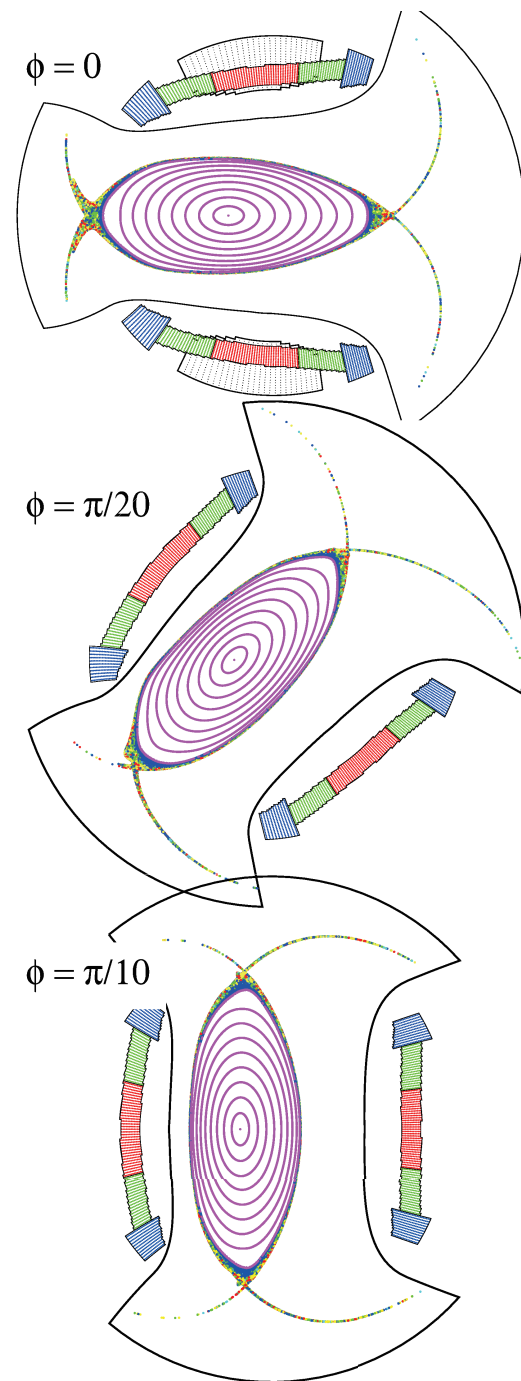


Fig. 9 Magnetic field configuration produced by the folded thin and flat helical coils shown in Fig. 8. Although the current density of HC-I is reduced compared to the case of Fig. 5, sufficient blanket space  $\delta$  and plasma volume are realized.

in the core plasma region. The peripheral region has high magnetic shear. The trapped orbits diagram (TPOD) [11] in Fig. 7 shows that the trapped particle orbit stays near the magnetic surface and the loss cone depth  $D_{lc}$  is very shallow. Thus, the performance of the high-energy particle confinement is comparable to the inner shift magnetic axis configuration of the LHD.

Table 2 Coil parameters for the case of Fig. 9 with  $R_0 = 16.7$  m and  $B_{ax} = 5$  T. ( $\delta$ : blanket space,  $V_{lcfs}$ : plasma volume).

	HC-I	HC-II	HC-III	$\delta / V_{lcfs}$
$I$ (MA)	53.5	-26.8	12.7	1.196 m
$J_c$ (A/mm <sup>2</sup> )	66.3	-30.2	15.1	1674 m <sup>3</sup>

The characteristics of the magnetic configurations shown in Figs. 5-7 are excellent. However, the coil current density of HC-I shown in Table 1 is very high compared to the values of LHD's helical coil.

To decrease the coil current density, we extended the coil height. Furthermore, the coil ends are folded as shown in Fig. 8 to mitigate the interference between coil end and divertor leg. A numerical example of this coil system is shown in Fig. 9. As shown in Table 2, the coil current density ( $J_c = 66.3$  A/mm<sup>2</sup>) of the center block HC-I is reduced as compared with the value shown in Table 1.

#### 4. Summary

We have proposed a thin and flat helical coil system with current distribution control. A helical coil is divided into three blocks parallel to each other. Therefore, we can change the magnetic surface form to the racetrack-type. Large blanket space and large plasma volume become compatible by adjusting the combination of helical coil current values.

Highly symmetric magnetic surfaces with divertor

legs, which turn to the back of the helical coils, are confirmed. Moreover, the confinement performance for high-energy particles is excellent.

The biggest problem in the proposed method is that the current density of center block becomes high to balance the large blanket space and large plasma volume. Another problem is the current reversal between the blocks of the helical coils. The stability of the critical current density at this configuration is part of a future study. Furthermore, the study the optimal helical coil shape for the reduced size helical fusion reactor is interesting.

The authors thank the members of the Meeting on Helical Reactor Design at the National Institute for Fusion Science for discussions regarding helical reactor systems. This work was performed with the support and under the auspices of the NIFS Collaborative Research Programs NIFS13KNST062.

- [1] A. Sagara *et al.*, Fusion Eng. Des. **87**, 594 (2012).
- [2] A. Sagara *et al.*, J. Nucl. Mater. **248**, 147 (1997).
- [3] T. Goto *et al.*, Nucl. Fusion **51**, 083045 (2011).
- [4] N. Ohya *et al.*, Nucl. Fusion **34**, 387 (1994).
- [5] Y. Kozaki *et al.*, Nucl. Fusion **49**, 115011 (2009).
- [6] N. Yanagi *et al.*, Plasma Fusion Res. **5**, S1026 (2010).
- [7] T. Watanabe, Plasma Fusion Res. **7**, 2403113 (2012).
- [8] M. Yokoyama *et al.*, Nucl. Fusion **40**, 261 (2000).
- [9] A.H. Boozer, Phys. Fluids **23**, 904 (1980).
- [10] L.P. Ku and A.H. Boozer, Nucl. Fusion **50**, 125005 (2010).
- [11] T. Watanabe, Plasma Fusion Res. **8**, 2403072 (2013).